RSC Advances

ROYAL SOCIETY OF CHEMISTRY

www.rsc.org/advances

Cite this: DOI: 10.1039/c0xx00000x

www.rsc.org/xxxxxx

ARTICLE TYPE

Development of a cell permeable ratiometric chemosensor and biomarker for hydrogen sulphate ions in aqueous solution

Buddhadeb Sen,[a] Manjira Mukherjee,[a] Siddhartha Pal,[a] Sushil Kumar Mandal,[b] Maninder S. Hundal,[c] Anisur Rahman Khuda-Bukhsh,[b] and Pabitra Chattopadhyay*[,a]

Received (in XXX, XXX) Xth XXXXXXXXX 20XX, Accepted Xth XXXXXXXXX 20XX
DOI: 10.1039/b000000x

A newly designed organic moiety, *5H-5,7a,12-triaza-dibenzo[a,e]azulen-6-one* (**L**) containing a seven membered ring behaves as a hydrogen sulphate ions selective ratiometric chemosensor. The formulation and detailed structural characterisations of **L** have been established using physico-chemical, spectroscopic tools and single crystal X-ray diffraction study. On additions of hydrogen sulphate ions to the solution of **L** in HEPES buffer (1 mM; water:ethanol (v/v), 98:2) at 25 °C at biological pH, a new fluorescence peak generated at 483 nm was increased with concomitant decrease of the weak fluorescence of **L** at 430 nm through an isoemissive point at 449 nm due to the selective binding of HSO_4^- ions with **L** in a 1 : 1 ratio with a binding constant (K) of 4.13 x 10^6 M^{-1}, and detects HSO_4^- ions as low as 5.5×10^{-7} M. The ratiometric enhancement of the fluorescence is based on intermolecular hydrogen bonding assisted chelation enhanced fluorescence (CHEF) process which has been evidenced by ^{1}HNMR titration and supported by theoretical (DFT) calculations. The probe (**L**) having no cytotoxic effect is also useful for the detection of intracellular HSO_4^- concentrations under a fluorescence microscope.

Introduction

Anions play a vital role in a wide range of industrial, agricultural, biological systems and environmental processes.[1] Thus, the design and development of selective optical chemosensors for various anions have gained considerable attention.[2] Among the various anions, hydrogen sulfate (HSO_4^-) ions dissociate at high pH to generate toxic sulfate (SO_4^{2-}), causing irritation of the skin and eyes and even respiratory paralysis. Despite its crucial roles in biological processes, only few examples of sensors for HSO_4^- have been reported.[3-4] Among all these sensors, most of them performed through single point detection[3] and only few acted upon ratiometric titration[4], but none of them as a cell permeable sensor for hydrogen sulphate in aqueous solvent has been reported. However, it is well known that ratiometric responses are more attractive because the ratio between the two emission intensities can be used to measure the analyte concentration and provide a built-in correction for environmental effects and stability under illumination.[5-6] So, it is a challenge for a chemist to develop a ratiometric water soluble cell permeable fluorescent probe for hydrogen sulfate ions.

Chemosensors based on anion-induced changes in fluorescence are particularly attractive because of the simplicity, high spatial and temporal resolution of fluorescence.[7] Secondary amides have been employed widely as hydrogen bond donor groups to bind anionic species.[8] The first example of a synthetic anion receptor containing secondary amides was reported by Pascal and co-workers in 1986.[9] Among the various types of these receptors, imidazolium based receptors have also been extensively investigated in recent years.

In the search of a water soluble HSO_4^- ions selective chemosensor, we designed and synthesized a new compound (**L**) in a facile route using imidazolium based secondary amides. **L** behaves as a ratiometric amplified chemosensor highly selective and sensitive fluorescent probe for sensing for HSO_4^- ions in HEPES buffer (1 mM, pH 7.4; 2% EtOH) at 25 °C upto a very low concentration (5.5×10^{-7} M) of HSO_4^- ions. This probe (**L**) was also useful to detect the presence of bisulphate ions in by acquiring image of HeLa cells under a fluorescence microscope and **L** has no cytotoxicity. To the best of our knowledge so far, the *5H-5,7a,12-triaza-dibenzo[a,e]azulen-6-one* (**L**) containing a seven membered ring as a water soluble cell permeable ratiometric fluorescent probe for hydrogen sulfate ions is still unexplored.[3-4]

Experimental section

Materials and methods

High-purity HEPES [*4-(2-hydroxyethyl)-1-piperazineethane-sulfonic acid*], *2-(2-aminophenyl)benz-imidazole*, *2-chloroacetyl chloride*, and *tetra butyl ammonium hydrogen sulphate* were purchased from Sigma Aldrich (India), solvents used were spectroscopic grade. Other chemicals, tetrabutyl ammonium salts of fluoride, chloride, bromide, iodide, acetate, dihydrogen phosphate and sodium salt of monohydrogen phosphate, azide, thiocyanate and nitrate were of analytical reagent grade and used without further purification except when specified. Milli-Q, 18.2 MΩ cm^{-1} water was used throughout all

experiments. A Shimadzu (model UV-1800) spectrophotometer was used for recording electronic spectra. FTIR spectra were recorded using Prestige-21 SHIMADZU FTIR spectrometer preparing KBr disk. ^{1}HNMR spectrum of organic moiety was obtained on a Bruker Avance DPX 500 MHz spectrometer using DMSO-d_6 solution. Electrospray ionization (ESI) mass spectra were recorded on a Qtof Micro YA263 mass spectrometer. A Systronics digital pH meter (model 335) was used to measure the pH of the solution and the adjustment of pH was done using either 50 mM HCl or sodium hydroxide solution. Steady-state fluorescence emission and excitation spectra were recorded with a Hitachi F-4500 FL Spectrophotometer. Time-resolved fluorescence lifetime measurements were performed using a HORIBA JOBIN Yvon picosecond pulsed diode laser-based time-correlated single-photon counting (TCSPC) spectrometer from IBH (UK) at λ_{ex}= 377 nm and MCP-PMT as a detector. Emission from the sample was collected at a right angle to the direction of the excitation beam maintaining magic angle polarization (54.71). The full width at half-maximum (FWHM) of the instrument response function was 250 ps, and the resolution was 28.6 ps per channel. Data were fitted to multiexponential functions after deconvolution of the instrument response function by an iterative reconvolution technique using IBH DAS 6.2 data analysis software in which reduced w2 and weighted residuals serve as parameters for goodness of fit.

Synthetic procedures

Synthesis of *[5H-5,7a,12-triaza-dibenzo[a,e]azulen-6-one]* (L)

2-chloroacetyl chloride (5.31 ml) was dissolved in chloroform (5 ml) and then added dropwise to an ice cold solution of *2-(2-aminophenyl)benzimidazole* (4.1848 g, 20 mmol) and Et_3N (3.0 ml) in chloroform (10 ml) very slowly with stirring. After being stirred for 4 h at room temperature, the mixture was removed under reduced pressure to obtain a white solid, which was filtered out and extracted with dichloromethane to afford compound 1.[10] In the next step, compound **1** was taken in dry acetonitrile having anhydrous K_2CO_3 and refluxed for 4 h. The volume of the solution was reduced to obtain a solid and then extracted with dichloromethane and finally purified by silica gel column chromatography using dichloromethane as the eluent (Scheme-1).

L. $C_{15}H_{11}N_3O$. Anal. Found: C, 72.52; H, 4.39; N, 17.01; Calc.: C, 72.28; H, 4.45; N, 16.86; IR (KBr, cm^{-1}): $\nu_{C=O}$, 1687, ν_{N-H}, 3205. (see ESI†); ^{1}H NMR (400 MHz, DMSO-d6): 10.637 (s, 1H), 8.087 (dd, 1H), 7.824 (dd, 1H), 7.745 (dd, 1H), 7.574 (q, 1H), 7.377-7.266 (m, 4H), 4.946 (s, 2H, -CH_2-CO); ESI-MS m/z 249.98 [M+H$^+$, 100%]; Calc.: 250.09; [M + H]$^+$; ^{13}C NMR (DMSO-d6): 166.332, 149.161, 137.348, 133.602, 131.465, 126.226, 126.041, 124.957, 118.106, 115.203, 46.215. Yield: 78 %.

Synthesis of compound 2 (L-HSO_4^-)

A 2.0 ml ethanolic solution of *tetra butyl ammonium hydrogen sulphate* (67.906 mg, 0.20 mmol) was added slowly to the stirred 8.0 ml solution of **L** (50 mg; ~ 0.20 mmol) in EtOH and the stirring was continued for 4.0 h. The resulting greenish coloured reaction mixture was filtered and kept aside for several days to get the solid product on slow evaporation at room temperature. The solid was so obtained and dried in vacuo for performing the characterization.

Compound **2**. $Bu_4N[C_{15}H_{12}N_3O_5S]$: $C_{31}H_{48}N_4O_5S$. Anal. Found: C, 63.53; H, 8.08; N, 9.74; S, 5.19; Calc.: C, 63.24; H, 8.22; N, 9.52; S, 5.45; IR (KBr, cm^{-1}): $\nu_{C=O}$, 1643, ν_{O-H}, 3422; $\nu_{S=O}$ 1113. ^{1}H NMR (400 MHz, DMSO-d_6): 11.060 (s, 1H), 8.212 (dd, 1H), 8.146 (dd, 1H), 7.948-7.916 (m, 1H), 7.798 (q, 1H), 7.716 (m, 2H), 7.520 (q, 1H), 7.448 (dd, 1H), 5.195 (s, 2H, -CH_2-CO), and for Bu_4N:[11] 3.209(m, 4CH_2) 1.607(m, 4CH_2) 1.340(m, 4CH_2), 0.970(t, 4CH_3) (see ESI†); ESI-MS: [M - Bu_4N^+ +H$^+$ + Na^+]$^+$, m/z, Found, 369.97, Calc.: 370.05; ^{13}C NMR (DMSO-d6): 166.346, 149.201, 137.506, 133.612, 131.474, 126.003, 125.667, 125.057, 117.960, 115.223, 46.325.

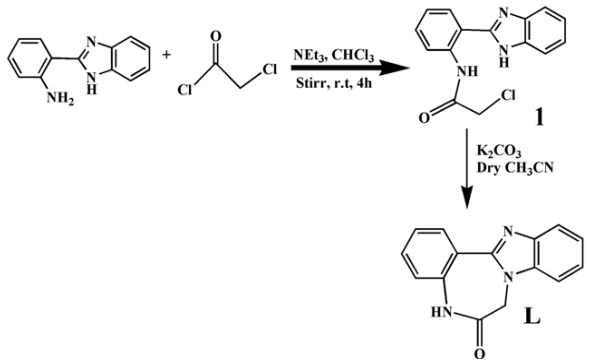

Scheme 1 Synthetic strategy of **L**

X-Ray crystallography

X-ray data of the suitable crystal of **L** was collected on a Bruker's Apex-II CCD diffractometer using MoKα (λ = 0.71069). The data were corrected for Lorentz and polarization effects and empirical absorption corrections were applied using SADABS from Bruker. A total of 12449 reflections were measured out of which 3426 were independent and 2801 were observed [I > 2σ(I)] for theta (θ) 1.66 to 28.19°. The structure was solved by direct methods using SIR-92 and refined by full-matrix least squares refinement methods based on F^2, using SHELX-97.[12] All calculations were performed using Wingx package.[13,14] Important crystallographic parameters are given in Table S1†. The crystallographic data of HL.NO_3 have been deposited to Cambridge Crystallographic Data Centre bearing the CCDC no. of 972698.

General method of UV-vis and fluorescence titration

Path length of the cells used for absorption and emission studies was 1 cm. For UV-vis and fluorescence titrations, stock solution of **L** was prepared in HEPES buffer (1 mM, pH 7.4; 2% EtOH) at 25 °C. Fluorescence measurements were performed using 5 nm x 5 nm slit width. All the fluorescence and absorbance spectra were taken after 30 minutes of mixing of HSO_4^- and **L**.

Preparation of cell and *in vitro* cellular imaging with L

Human cervical cancer cell, HeLa cell line was purchased from National Center for Cell Science (NCCS), Pune, India and was used throughout the study. Cell were cultured in Dulbecco's modified Eagle's medium (DMEM, Gibco BRL) supplemented with 10% FBS (Gibco BRL), and 1% antibiotic mixture containing penicillin, streptomycin and neomycin (PSN, Gibco BRL), at 37 °C in a humidified incubator with 5% CO_2. For experimental study, cells were grown to 80-90 % confluence, harvested with 0.025 % trypsin (Gibco BRL) and 0.52 mM EDTA (Gibco BRL) in PBS (phosphate-buffered saline, Sigma

Diagnostics) and plated at desire cell concentration and allowed to re-equilibrate for 24h before any treatment. Cells were rinsed with PBS and incubated with DMEM-containing **L** (10 μM, 1% DMSO) for 30 min at 37 °C. All experiments were conducted in DMEM containing 10% FBS and 1% PSN antibiotic. The imaging system was composed of a fluorescence microscope (ZEISS Axioskop 2 plus) with an objective lens [10×].

Cell cytotoxicity assay

To test the cytotoxicity of **L**, MTT [*3-(4,5-dimethyl-thiazol-2-yl)-2,S-diphenyl tetrazolium bromide*] assay was performed with the help of the procedure described earlier.[15] After treatments of the probe (5, 10, 20, and 50 μM), 10μl of MTT solution (10mg/ml PBS) was added in each well of a 96-well culture plate and incubated continuously at 37°C for 6 h. All mediums were removed from wells and replaced with 100μl of acidic isopropanol. The intracellular formazan crystals (blue-violet) formed were solubilized with 0.04 N acidic isopropanol and the absorbance of the solution was measured at 595 nm wavelength with a microplate reader. Values are means ± S.D. of three independent experiments. The cell cytotoxicity was calculated as percent cell cytotoxicity = 100% cell viability.

Result and discussion

Synthesis and structural characterisation

Organic moiety was synthesized by the reaction of *2-(2-aminophenyl)benzimidazole* with *2-chloroacetyl chloride* in chloroform solvent followed by ring closer step (Scheme 1) and characterised by physico-chemical and spectroscopic tools (Figs. S1a-S1d†). The FTIR spectrum of **L** contains bands for the C=O and NH groups at 1687 and 3205 cm^{-1}, respectively along with other characteristic peaks for benzimidazole unit (Fig. S1a in ESI†). The QTOF-ESI+ spectrum of **L** contains molecular ion peak at m/z 249.98 corresponding to $[L+H^+]$ (Fig. S1c, ESI†). The well-resolved ^1H NMR spectrum of **L** is in support of the formulation and the structure established by single crystal X-ray crystallographic analysis of $HL.NO_3$.

The solid L-HSO_4^- ensembled species (**2**) was obtained from the reaction of *tetra butyl ammonium hydrogen sulphate* with methanolic solution of **L** in 1:1 mole ratio at stirring condition. The ESI mass spectrum of **2** in methanol shows a molecular-ion peak at m/z 369.97 with ~14% abundance, which can be assigned to $[M - Bu_4N^+ + H^+ + Na^+]^+$ (calculated value at m/z, 370.05). A characteristic peak for $\nu_{S=O}$ at 1113 cm^{-1} in the FTIR spectrum of **2** confirms the existence of sulphate ion attached to **2**.[16] The ^{1}HNMR spectrum obtained in DMSO-d_6 confirmed the presence of the **L** bound to HSO_4^- ions (Figs. S2a-S2d†).

Single crystals of the probe (**L**) were obtained as $HL.NO_3$ from the methanolic solution of **L** in presence of aq. sodium nitrate. The $HL.NO_3$ crystallizes in the triclinic space group $P\bar{1}$. An ORTEP view of the probe with atom labelling scheme is illustrated in Fig. 1, and a selection of bond distances and angles is listed in Table S2†. The bond distance C1-N1 (1.3557(18) Å) or C11-N1 (1.4114(17) Å) is somewhat longer than that of any bond of C8-N3 (1.3887(18) Å) or C8-N3 (1.3455(17) Å) due to the single bond character of C1-N1 or C11-N1 and sp3 hybridisation of N1. In the same way, the longer bond distance (1.4602(18) Å) is also indicative of the single bond character of C2-N2 bond. The crystal structure of **L** is stabilized by the presence of the nitrate anion as counter anion for balancing the produced charge of HL^+ formed due to the protonation of N(3) atom.

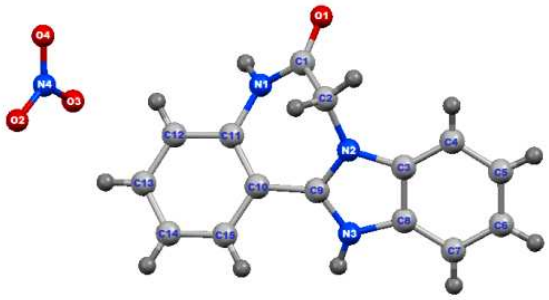

Fig. 1 A molecular view with atom numbering scheme of $HL.NO_3$ (50% ellipsoid probability).

UV-vis spectroscopic studies of L in presence of HSO_4^-

UV-vis spectra of **L** was recorded in HEPES buffer (1 mM, pH 7.4; 2% ethanol) at 25 °C shows an absorption maximum at 383 nm which may possibly be attributed to the intramolecular charge transfer (CT) transition. The absorption intensity of **L** at 383 nm gradually decreased, accompanied by the formation of a new absorption peak at 425 nm (Fig. 2) as the addition of HSO_4^- ions was increased stepwise (0-20 μM) with an isosbestic point at 402 nm and the solution turned from colourless to faint greenish yellow (Fig. S3†).

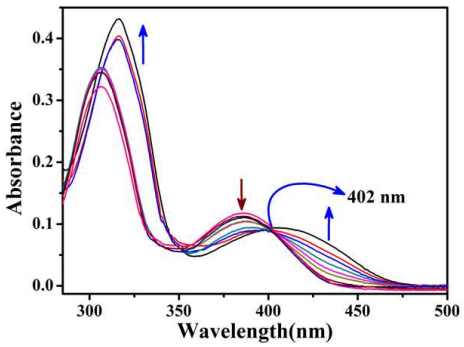

Fig. 2 UV-vis titration spectra of **L** (10 μM) upon incremental addition of HSO_4^- ions (0-20 μM) in HEPES buffer (1 mM, pH 7.4; 2% EtOH) at 25 °C.

Emission study

Organic moiety (**L**) showed emission spectrum at 430 nm in HEPES buffer (1 mM, pH 7.4; 2% ethanol) at 25 °C excited at 383 nm considering the absorption at 383 nm (Fig. S4†). Fluorescence quantum yields (Φ) were estimated by integrating the area under the fluorescence curves with the equation:

$$\Phi_{sample} = \Phi_{ref} \times \frac{OD_{ref} \times A_{sample} \times \eta^2_{sample}}{OD_{sample} \times A_{ref} \times \eta^2_{ref}}$$

where A is the area under the fluorescence spectral curve and OD is optical density of the compound at the excitation wavelength, 383 nm, η is the refractive index of the solvent used.

The standard used for the measurement of fluorescence quantum yield was anthracene (Φ = 0.29 in ethanol). This emission property of the probe (**L**) has not been affected over the pH range 4.0 to 10.0 (Fig. S5†).

Fluorescence studies of L in presence of HSO_4^- ions

The emission property of **L** in presence of various concentrations of HSO_4^- ions was verified. On addition of various concentrations of HSO_4^- ions (0-20 μM), fluorescence intensity at 430 nm was significantly decreased with a concomitant increase of intensity at 483 nm through an isoemissive point at 449 nm (Fig. 3). The fluorescence quantum yield has also been calculated in absence and presence of HSO_4^- ions. And from this measurement it is clear that the fluorescence quantum yield in presence of HSO_4^- (Φ = 0.45) increases ~4 times than that of free **L** (Φ = 0.12). This spectral feature for the addition of HSO_4^- ions was also supported by the fluorescence color change from blue to green in presence of UV light (Fig. S6†).

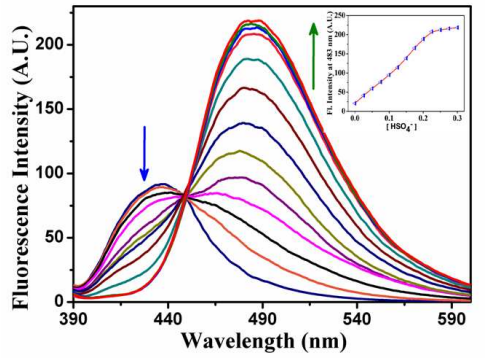

Fig. 3 Emission spectra of **L** in presence of HSO_4^- (0-20 μM) at λ_{ex} = 383 nm in HEPES buffer (1 mM, pH 7.4; 2% EtOH) at 25 °C.

Ratiometric signaling of fluorescence output at two different wavelengths plotted as a function of concentration of HSO_4^- indicates that the fluorescence intensity ratio of wave length 483 nm and 430 nm (I_{483}/I_{430}) gradually increases with increase of the concentration of HSO_4^- ions (Fig. S7†) and after a certain time it level up producing a sigmoid curve. **L** exhibited a near about 14-fold increase of its fluorescence intensity upon addition of only 2.0 equivalent of HSO_4^- ions. The detection limit was determined and was found to be 5.5 x10^{-7} M^{-1} (Fig. S8†), which is significantly low. Interestingly, the introduction of other anions does not intefere the fluorescence enhancement. The fluorescence characteristics of **L** (10 μM) were observed upon the addition of excess 50 equivalents of different anions *i.e.* F^-, Cl^-, Br^-, I^-, CN^-, N_3^- NO_3^-, ClO_4^-, $H_2PO_4^-$, HPO_4^{2-}, PO_4^{3-}, $H_2AsO_4^-$, $HAsO_4^{2-}$, AsO_3^{3-}, OAc^-, SO_4^{2-}, S^{2-}, and HSO_4^- but only HSO_4^- selectively enhance the fluorescence intensity of **L** system (Fig. 4). In presence of 10 times excess of various tested anions together with **L** and HSO_4^-, almost no adverse effect on intensity was observed (Fig. S9†).

The compound formed between **L** and HSO_4^- is found to be 1:1 in stoichiometry, which was established with the help of Job's plot (Fig. S10†) using the fluorescence study. This 1:1 stoichiometric ratio is also supported by the physico-chemical and spectroscopic data of the **L**-HSO_4^- ensemble species isolated in the solid form.

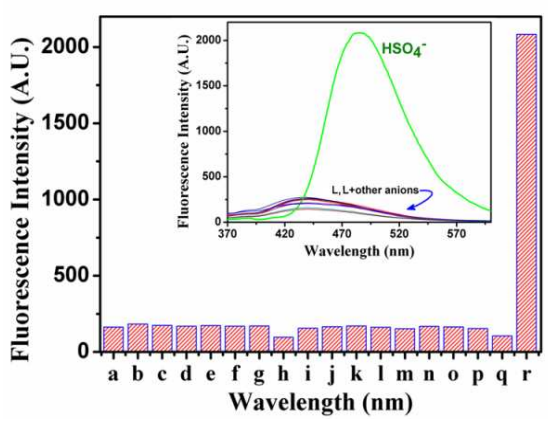

Fig. 4 Anion selectivity of **L** in presence of different anions in HEPES buffer (1 mM, pH 7.4; 2% EtOH) at 25 °C where a)**L**, b) F^-, c) Cl^-, d) Br^-, e) I^-, f) CN^-, g) N_3^-, h) NO_3^-, i) ClO_4^-, j) $H_2PO_4^-$, k) HPO_4^{2-}, l) $H_2AsO_4^-$, m) $HAsO_4^{2-}$, n) AsO_3^{3-}, o) OAc^-, p) SO_4^{2-}, q) S^{2-} and r) HSO_4^- at λ_{em}= 483nm.

To ensure the formation of the **L**-HSO_4^- species in solution state, ^{1}H NMR titration was also performed in dmso-d_6. Fig. 5 clearly indicates the interaction of amide N-H proton with which HSO_4^- as the signal due to this proton shifted to downfield (δ value from 10.637 ppm to 11.060 ppm) and the protons of -CH_2 of the seven membered ring also shifted to higher δ value from 4.946 ppm to 5.195 ppm along with a significant shifting of H^c towards downfield by Δδ of 0.388 ppm (Δδ = 8.212 - 7.824 ppm, Fig. S11†) on gradual addition of HSO_4^- ions.

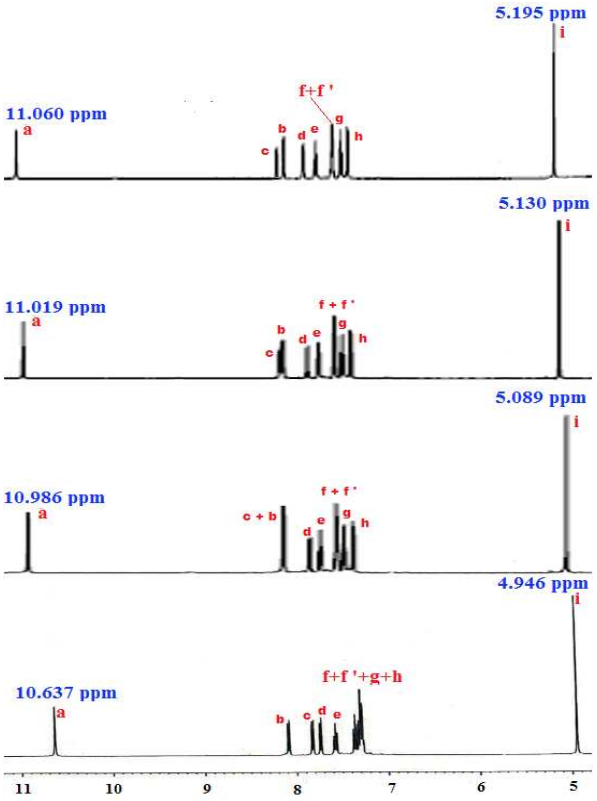

Fig. 5 Partial ^{1}H NMR spectra for **L** (10 mM) in presence of varying [HSO_4^-] [A) 0 mM, B) 3.33 mM, C) 6.67 mM, and D) 10 mM] in DMSO-d_6 [for clarity, expanded region of 7.2 to 8.3 ppm of ^{1}HNMR spectra in Fig. S11†]

The binding constant value was determined from the emission intensity data following the modified Benesi-Hildebrand equation.[17,18]

$$1/(F_X-F_0)=1/(F_{max}-F_0)+(1/K[C])(1/(F_{max}-F_0))$$

where F_0, F_X, and F_∞ are the emission intensities of organic moiety considered in the absence of HSO_4^- ions, at an intermediate HSO_4^- concentration, and at a concentration of complete interaction, respectively, and where K is the association constant and [C] is the concentration of HSO_4^-. K value (4.13 x 10^6 M^{-1}) was calculated from the slope/ intercept using the plot of $(F_\infty-F_0)/(F_x-F_0)$ against $1/[HSO_4^-]$ (Fig. S12†). This value of binding constant is the indication of strong binding affinity of the organic moiety towards the HSO_4^- ions. In the fluorescence average life time measurement the life time of **L** was found to be 5.77 ns at λ_{em}= 483 nm. After gradual addition of HSO_4^- to the solution of **L**, the average lifetime of the **L**-HSO_4^- species (at λ_{em}= 483 nm) increased from 11.79 ns (when **L** : HSO_4^-; 1 : 0.5) to 12.15 ns (when **L** : HSO_4^- ; 1 : 1), and it is clearly ascribed by the intermolecular hydrogen bonding assisted CHEF process (Table S3†)(Fig. 6). The strong binding of HSO_4^- ion with organic moiety (**L**), is evidenced by the significant binding constant value (4.13 x 10^6 M^{-1}) and this phenomenon played a key role to deter the PET process in support of the selective detection of HSO_4^- ions through fluorescence enhancement (Scheme 2).

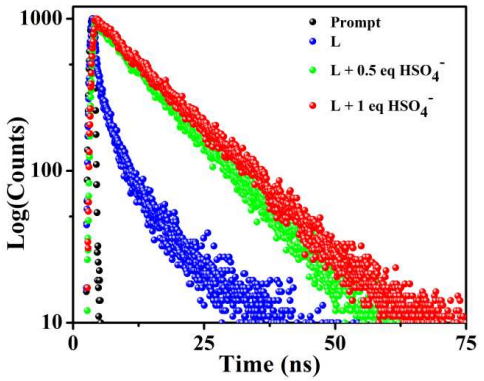

Fig. 6 Time resolved fluorescence decay of **L** (10μM) only and in presence of added HSO_4^- in HEPES buffer (1 mM, pH 7.4; 2% EtOH) at 25 °C using a nano LED of 377 nm as the light source at λ_{em} = 483nm.

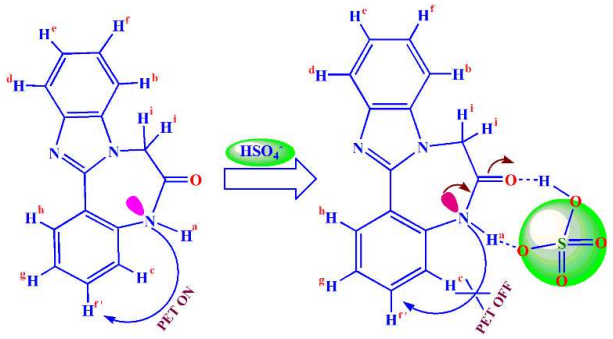

Scheme 2 Proposed mechanism of fluorescence enhancement of receptor (**L**) in presence of HSO_4^- ions.

According to the equations: [19] $\tau^{-1} = k_r + k_{nr}$ and $k_r = \Phi_f/\tau$, the radiative rate constant k_r and total nonradiative rate constant k_{nr} of organic moiety, **L** and HSO_4^- complex with **L** were listed in Table S3†. The data suggest that k_{nr} has just slightly changed but the factor that induces fluorescent enhancement is mainly ascribed to the increase of k_r.

Geometry optimization

To clarify the configurations and H-bonding feature of the host (**L**) and guest-host species (**2; L**-HSO_4^-), DFT calculations were performed using **Gaussian-09** software over a Red Hat Linux IBM cluster. Molecular level interactions between **L** and **2** have been studied using density functional theory (DFT) with the **B3LYP/6-31G(d)** functional model and basis set.

To assure the mode of interaction of the probe (**L**) with HSO_4^- ions either in ring or chain fashion, the optimised geometries in both fashions were obtained by theoretical calculation (Fig. S13†). From the calculation of energy of HOMO and LUMO in this study, it is indicated that the binding mode of the guest (HSO_4^- ion) with the host (**L**) through ring is more preferable than that through chain. In case of ring structure, the energy gap between HOMO-LUMO is 3.77 eV which is lower than that of free **L** (4.53 eV) (Table S4†). Here, charge distribution of HOMO in compound **2** confirms that the most of the charge is on HSO_4^- ion attached with N-H through H-bonding (Fig. 7).

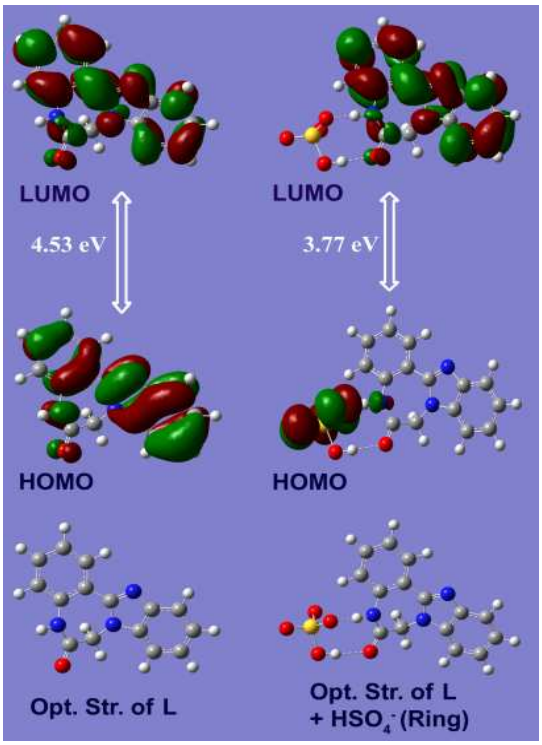

Fig. 7 Optimized structures of **L** and **L**-HSO_4^- species.

Biological studies of L in presence of HSO_4^-

To examine the utility of the probe in biological systems, it was applied to human cervical cancer HeLa cell. In these experiments both the **L** and HSO_4^- was allowed to uptake by the cells of

interest and the images of the cells were recorded by the fluorescence microscopy following excitation at ~383 nm. After incubation with **L** (10 μM) for 30 min, the cells displayed very faint intracellular fluorescence. However, cells exhibited intensive fluorescence when exogenous HSO_4^- was introduced into the cell via incubation with Bu_4NHSO_4 (Fig. 8). The fluorescence responses of the probe with various concentrations of added HSO_4^- are clearly evident from the cellular imaging. In addition, the *in vitro* study showed that 10 μM of **L** did not show no cytotoxic effect to cell upto 6 h (Fig. S14†). These results indicate that the probe has a huge potentiality for both *in vitro* and *in vivo* application as HSO_4^- sensor as well as imaging in different ways as same manner for live cell imaging.

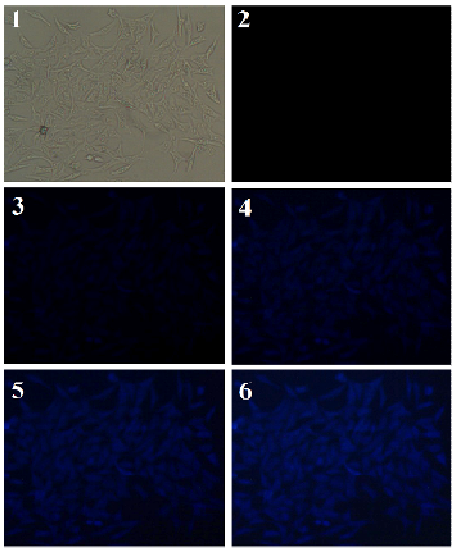

Fig. 8 Fluorescence image of HeLa cells after incubation with **L** in presence of hydrogen sulphate ions 1)Phase Contrast, 2) 0 μM, 3) 3 μM, 4) 5 μM, 5) 7 μM, 6) 10 μM for 30 min at 37 °C and the samples were excited at λ= 383 nm.

Conclusions

In conclusion, a water soluble dual receptor for HSO_4^- ions was synthesized by a facile two-step process. The formulation and detailed structural characterisations has been established using physico-chemical and spectroscopic tools along with detailed structural analyses by single crystal X-ray crystallography. The fluorimetric and titrimetric titration of **L** by adding HSO_4^- ions in HEPES buffer (1 mM, pH 7.4; 2% ethanol) at 25 °C showed that **L** is very specific and sensitive chemosensor for HSO_4^- ions. On addition of HSO_4^- ions, the emission intensity at 430 nm of free **L** decreases gradually with the generation of a new peak at 483 nm through an isoemissive point at 449 nm due to the hydrogen bonding formation between the amide hydrogen and bisulphate ion. This interaction was also clearly supported by ^{1}HNMR titration and theoretical DFT calculation. Interestingly, this probe could be considered as a potent probe for HSO_4^- ions because the fluorescence enhancement at λ_{em} = 483 nm of bio-friendly visible region is taken place in a more attractive ratiometric response fashion with almost no interference by the biologically relevant anions in green solvent. This probe has been successfully used as biomarker of bisulphate ions as **L** is significantly efficient to detect the distribution of hydrogen sulphate ions *in vitro* in living cells (HeLa) in aqueous medium at biological pH by developing the good image.

Acknowledgments

Financial assistance from CSIR, New Delhi, India is gratefully acknowledged. B. Sen wishes to thank to UGC, New Delhi, India for offering him the fellowship. The authors sincerely acknowledge Prof. Samita Basu and Mr. Ajay Das, Chemical Science Division, SINP, Kolkata for enabling TCSPC instrument, and Prof. B. Mukhopadhyay, IISER, Kolkata for providing the facility to record some ^{1}H NMR spectra and Mr. Samya Banerjee, IISC, Bangalore for ^{13}C NMR spectra.

Notes and references

[a] *Department of Chemistry, The University of Burdwan, Golapbag, Burdwan 713104, India. E-mail: pabitracc@yahoo.com*
[b] *Molecular Biology and Genetics Laboratory, Department of Zoology, Kalyani University, India*
[c] *Department of Chemistry, Guru Nanak Dev University, Amritsar 143005, India*

† Electronic Supplementary Information (ESI) available: [Experimental section, tables, schemes, figures, characterization data, and some spectra], See *DOI: 10.1039/b000000x/*

‡ CCDC no for $HL.NO_3$ is 972698.

Corresponding Author
* E-mail: pabitracc@yahoo.com. Tel: +91-342-2558554 extn. 424. Fax: +91-342-2530452.

1 (a) T.Y. Joo, N. Singh, G.W. Lee and D.O. Jiang, *Tetrahedron Lett.*, 2007, **48**, 8846; (*b*) J.M. Hermida-Ramon and C.M. Estevez, *Chem. Eur. J.*, 2007, **13**, 4743; (c) Y. Michigami, Y. Kuroda, K. Ueda and Y. Yamamoto, *Anal. Chim. Acta*, 1993, **274**, 299; (*d*) P.A. Gale, *Acc. Chem. Res.*, 2006, **39**, 465; (*e*) E.A. Katayev, Y.A. Ustynyuk and J.L. Sesser, *Coord. Chem. Rev.*, 2006, **250**, 3004; (*f*) F.P. Schmidtchen, *Coord. Chem. Rev.*, 2006, **250**, 2918; (*g*) V. Amendola, M. Bonizzoni, D. Esteban-G´omez, L. Fabbrizzi, M. Licchelli, F. Sancenon and A. Taglietti, *Coord. Chem. Rev.*, 2006, **250**, 1451; (*h*) J.M. Llinares,D. Powell and K. Bowman-James, *Coord. Chem. Rev.*, 2003, **240**, 57; (*i*) R. Martınez-Manez and F. Sancenon, *Chem. Rev.*, 2003, **103**, 4419.

2 (a) M.E. Moragues, R. Martinez-Manez and F. Sancenon, *Chem. Soc. Rev.,* 2011, **40**, 2593; (b) M.E. Moragues, R. Martınez-Manez and F. Sancenon, *Chem. Soc. Rev*., 2011, **40**, 2593; (c) A.F. Li, J.H. Wang, F. Wang and Y. B. Jiang, *Chem. Soc. Rev*., 2010, **39**, 3729; (d) R.M. Duke, E.B. Veale, F.M. Pfeffer, P.E. Kruger and T. Gunnlaugsson, *Chem. Soc. Rev*., 2010, **39**, 3936; (e) P.A. Gale, *Chem. Soc. Rev*., 2010, **39**, 3746; (f) E.J. O'Neil and B.D. Smith, *Coord. Chem.Rev.*, 2006, **250**, 3068; (g) R. Martinez-Manez and F. Sancenon, *Chem. Rev.,* 2003, **103,** 4419.

3 (a) U. Fegade, H. Sharma, K. Tayade, S. Attarde, N. Singh and A. Kuwar, *Org. Biomol. Chem.*, 2013, DOI: 10.1039/c3ob41291a; (b) Q. Li, Y. Guo and S. Shao, *Analyst*, 2012, **137**, 4497; (c) S.T. Yang, D.J. Liao, S.J. Chen, C. H. Hu and A. T. Wu, *Analyst*, 2012, **137**, 1553; (d) Q. Li, Y. Yue, Y. Guo and S. Shao*, Sensors and Actuators B: Chemical*, 2012, **173**, 797; (e) K. Kaur, V.K. Bhardwaj, N. Kaur and N. Singh, *Inorg. Chem. Commun.,* 2012, **18**, 79; (f) H.J. Kim, S. Bhuniya, R.K. Mahajan, R. Puri, H.G. Liu, K.C. Ko, J.Y. Lee and J.S. Kim, *Chem. Commun.*, 2009, 7128; (g) R. Shen, X.B. Pan, H.F. Wang, L.H. Yao, J.C. Wu and N. Tang, *Dalton Trans*., 2008, 3574

4 (a) J. Chang, Y. Lu, S. He, C. Liu, L. Zhao and X. Zeng, *Chem. Commun.,* 2013, **49**, 6259; (b) W.J. Xue, L. Li, Q. Li and A.X. Wu, Talanta, 2012, 88, 734; (c) A. Mallick, T. Katayama, Y. Ishibasi, M. Yasudab and H. Miyasaka, Analyst, 2011, **136**, 275.

5 Z. Xu, Y. Xiao, X. Qian, J. Cui, and D. Cui, *Org. Lett.,* 2005, **7**, 889.
6 B. Valeur, and I. Leray, *Coord. Chem. Rev.,* 2000, **205,** 3.
7 (a) J.S. Ma, L.N. Sobenina, A.I. Mikhaleva, G. Yang and B.A. Trofimov, Beilstein J. Org. Chem., 2011, 7, 46; (b) T. Gunnlaugsson, M. Glynn, G.M. Tocci, P.E. Kruger and F.M. Pfeffer, Coord. Chem.Rev., 2006, 250, 3094; (c) R. Martinez-Ma nez and F. Sancanon, Chem. Rev., 2003, 103, 4419; (d) J.F. Callan, A.P. de Silva and D.C. Magri, Tetrahedron, 2005, 61, 8551; (e) J. Zhao, T. M. Fyles and T.D. James, Angew. Chem. Int. Ed., 2004, 43, 3461; (f) C.H. Lee, H. Miyaji, D.W. Yoon and J.L. Sessler, Chem. Commun., 2008, 24; (g) S.K. Kim, D.H. Lee, J.I. Hong and J. Yoon, Acc. Chem. Res., 2009, 42, 23; (h) X. Huang, Z. Guo, W. Zhu, Y. Xie and H. Tian, Chem. Commun., 2008, 5143.
8 P.A. Gale, in The Encyclopedia of Supramolecular Chemistry, eds. J. L. Atwood and J. W. Steed, Dekker, New York, 2004, pp. 31-41.
9 R. A. Pascal, Jr, J. Spergel and D. Van Engen, *Tetrahedron Lett.*, 1986, **27**, 4099.
10 X. Zhou, P. Li, Z. Shi, X. Tang, C. Chen and W. Liu, *Inorg Chem.*, 2012, **51**, 9226.
11. B. Das, S. Sarkar, A. Patra, M.G.B. Drew and P. Chattopadhyay, *J. Coord. Chem.*, 2008, **61**, 1689.
12 A. Altomare, G. Cascarano, C. Giacovazzo and A. Guagliardi, *J. Appl. Crystallogr*., 1993, **26**, 343.
13 G.M. Sheldrick, *Acta Cryst A*, 2008, **64**, 112.
14 L.J. Farrugia, *J. Appl. Cryst.*, 1999, **32**, 837.
15 J. Ratha, K.A. Majumdar, S. K. Mandal, R. Bera, C. Sarkar, B. Saha, C. Mandal, K.D. Saha and R. Bhadra, *Mol. Cell Biochem*., 2006, **290**, 113.
16 J. Zhou, D.T. Moore, L. Wöste, G. Meijer, D.M. Neumark, K.R. Asmis, *J. Chem. Phys.*, 2006, **125**, 111102.
17 A. Mallick, B. Haldar, and N. Chattopadhyay, *Photochem. Photobiol*., 2005, **78**, 215.
18 H.A. Benesi and J.H. Hildebrand, *J. Am. Chem. Soc.*, 1949, **71**, 2703.
19 N.J. Turro, Modern Molecular Photochemistry; Benjamin/ Cummings Publishing Co., Inc.: Menlo Park, CA, 1978.

Graphical Abstract

A newly designed water soluble organic moiety, *5H-5,7a,12-triaza-dibenzo[a,e]azulen-6-one* (**L**) having a seven membered ring behaves as a cell permeable ratiometric chemosensor selectively for hydrogen sulphate ions of very low concentration of 5.5×10^{-7} M in aqueous solvent. Gradual additions of hydrogen sulphate ions to **L**, enhancement of a new fluorescent peak at 483 nm is obtained with the decrease of weak peak of free **L** at 430 nm through an isoemissive point at 449 nm was observed in HEPES buffer (1 mM; water : ethanol (v/v), 98:2) at 25°C at biological pH. This probe is an efficient biomarker for the detection of the distribution of bisulphate ions in living cells under a fluorescence microscope.